THE TOTAL PHOTOPRODUCTION CROSS SECTION AND ITS DECOMPOSITION

ALEXANDER V. FEDOTOV
ITEP, Moscow, Russia / DESY, Hamburg, Germany
on behalf of the H1 COLLABORATION

ABSTRACT

New preliminary results on γp scattering are reported as obtained with the H1 experiment at HERA based on 1994 data. The correlation between different sub-processes is measured. The total cross section is determined with a precision better than in earlier measurements at HERA.

1. Introduction

In low-angle ep scattering, $ep \rightarrow e'X$, one deals with a practically real photon interacting with the proton, the photon energy being $E_\gamma = E_e - E_{e'}$. The total γp cross section $\sigma_{tot}^{\gamma p}$ is then determined by a Weizsäcker-Williams-type formula [1]

$$d\sigma^{ep}(s)/dy|_{Q^2<Q^2_{max}} = F(y, Q^2_{max}) \cdot \sigma_{tot}^{\gamma p}(ys)$$

with "photon flux" given by

$$F = \frac{\alpha}{2\pi}\left[\frac{1+(1+y)^2}{y}\ln\frac{Q^2_{max}}{Q^2_{min}} - \frac{2(1-y)}{y}\left(1-\frac{Q^2_{min}}{Q^2_{max}}\right)\right] ,$$

where $s = (p_e + p_p)^2$, $y = 1 - E_{e'}/E_e$, $Q^2 = -(p_e - p_{e'})^2$, $Q^2_{min}(y) = (m_e y)^2/(1-y^2)$. Thus, ep scattering gives access to a study of γp interactions.

The commissioning of HERA ep collider in 1992 provided the first $\sigma_{tot}^{\gamma p}$ measurements by H1 [2] and ZEUS [3] collaborations at γp center of mass energy $W_{\gamma p}$ ~200 GeV. [1)] As compared to the earlier fixed-target data [4] at $W_{\gamma p}$ <20 GeV , these measurements established a moderate rise of $\sigma_{tot}^{\gamma p}$ with energy which is similar to that observed in hadron-hadron collisions.

In this paper, we present preliminary results of a new $\sigma_{tot}^{\gamma p}$ measurement with H1 detector based on 1994 data. The γp scattering may be decomposed into five channels

•	elastic diffraction	(EL)	:	$\gamma p \rightarrow Vp$, $V = \rho^0, \omega, \phi$
•	single γ diffraction	(GD)	:	$\gamma p \rightarrow M_X p$
•	single proton diffraction	(PD)	:	$\gamma p \rightarrow VM_X$, $V = \rho^0, \omega, \phi$
•	double diffraction	(DD)	:	$\gamma p \rightarrow M_{X1} M_{X2}$
•	non-diffractive = all the rest	(ND)	:	$\gamma p \rightarrow X$.

In the current analysis, we try not to make *a priori* assumptions on the contributions of the above channels, but rather measure them (a very loose assumption of σ_{DD} <40 μb is only left ultimately). This is made possible due to the usage of a dedicated trigger which was sensitive to all five channels. This, together with a better understanding of the H1 luminosity system, allows us to reduce the uncertainty in $\sigma_{tot}^{\gamma p}$ measurement as compared to the earlier HERA results .

[1)] A less precise flux formula was used in [2] which resulted in an underestimate of $\sigma_{tot}^{\gamma p}$ by 6-7%.

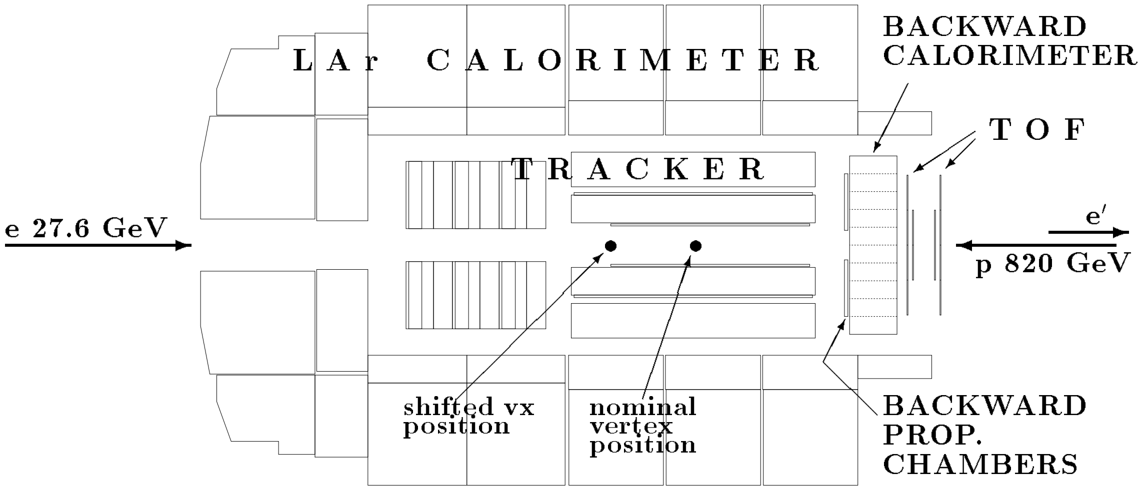

Figure 1: A scheme of the central part of H1 detector.

2. Detector, Trigger and Data Samples

A detailed description of the H1 detector can be found elsewhere [5]. Its central part with few sub-detectors relevant for the present analysis, is sketched in Fig.1 .

The data were taken in October 1994 when HERA operated in e^+p mode 27.6×820 GeV . The trigger required a coincidence of two main *trigger elements*.

The first trigger element was an electron detected in the electron tagger of the H1 luminosity system [6]. Located 33 m away from the main detector, the e-tagger detects electrons scattered to very low angles, corresponding to Q^2 <0.01 GeV^2 , and provides a measurement of y . In the working range of 0.3< y <0.7 , its acceptance to photoproduction events is known with a 5% accuracy. This range determines the c.m. energy interval $W_{\gamma p}$ =165–252 GeV with the average value of 197 GeV . In order to suppress a background from bremsstrahlung events $ep \to e'\gamma p$, this trigger element was activated only when there was no signal in the photon tagger — a small calorimeter 102 m away from the main detector.

The second trigger element was a signal in the time-of-flight scintillator system (TOF), see Fig.1 . The TOF covers quite low angles in γ-direction and provides a uniform efficiency of ∼70% to all five subprocesses of γp scattering, including the elastic one and p-diffraction.

Along with the photoproduction events, the trigger is also fired by accidental coincidences of different nature between the two trigger elements, their rate being few times larger than the physics rate. The majority of backgrounds are rejected off-line by additional selections. The remaining background contribution is well under control due to events recorded by auxiliary monitoring triggers switched on in parallel to the main trigger and based on TOF and e-tagger signals separately.

Two data sets were taken, each corresponding to luminosity of ∼24 nb^{-1}, or ∼20k physical events: one with a *nominal interaction-point position* and another with a *vertex shifted by 71cm* along the p-beam direction, as shown in Fig.1 . The shifted vertex sample is advantageous due to a higher acceptance to low-mass states produced in the γ-direction. On the other hand, the sample with nominal vertex has a substantially higher precision of luminosity measurement: 1.6% as compared to 5.6% in the first case. We analyse the two samples independently.

3. Method

In any kinematic domain $\Delta\tau$, the expected number of events is given by

$$N_{ev}(\Delta\tau) = k \sum_{i=1}^{5} \varepsilon_i(\Delta\tau) \cdot \sigma_i \tag{1}$$

where σ_i stands for the unknown total cross section of the i-th subprocess, $\varepsilon_i(\Delta\tau)$ — the corresponding y-averaged efficiency of (TOF-trigger-element $\cdot$ off-line-selections) which can be determined with Monte-Carlo, k being a constant accounting for luminosity $\mathcal{L}$, e-tagger acceptance $A(y)$ and flux factor F, $k = \mathcal{L} \cdot \int_{y_{min}}^{y_{max}} A(y) \cdot F(y)\, dy$.

Within appropriate kinematic regions, one could try to find all σ_i by fitting Eq.1 to data, then $\sigma_{tot}^{\gamma p}$ would be equal to $\sum \sigma_i$. However, we did not manage to achieve a sufficient sensitivity to separate all five channels. Therefore, we decided to extract the results as a function of σ_{DD}, which is fixed within the fit.

To calculate ε_i in Eq.1 , two different MC generators are used: PYTHIA 5.6 [7], and PHOJET [8] — a new γp generator based on dual parton model. As far as diffractive channels are concerned, the diffractive mass M_X is generated according to $d\sigma/dM_X^2 \sim 1/M_X^2$ in both programs, the 4-momentum transfered in the t-channel, t, has an exponential distribution e^{bt} . PHOJET is, however, a bit more elaborate, e.g., taking into account the resonance production and hard-scattering admixture. We extract the diffractive cross section unfolded to $x_{\mathbb{P}} = M_X^2/W_{\gamma p}^2 < 0.1$ region.

4. Results and Discussion

4.1 Shifted vertex sample

The basic off-line selections are either *a track* in the tracker *or a hit* in the backward proportional chambers (BPC), see Fig.1 . This effectively removes the background events, the remaining ~5% fraction of them subtracted by statistical methods. At the same time, the overall efficiencies ε_i are kept quite high:

channel	ND	GD	PD	DD	EL
ε	.61	.74	.68	.71	.57

We find in any event a "particle" with maximal value of pseudorapidity η by considering tracks, BPC-hits and clusters in LAr-calorimeter as "particles", the pseudorapidity $\eta = -\ln(\tan(\theta/2))$ calculated in lab. frame with respect to the p-beam direction. This defines the η_{max} variable. Similarly, the η_{min} variable is defined as the minimum η over "particles" with $\eta > -2.4$.

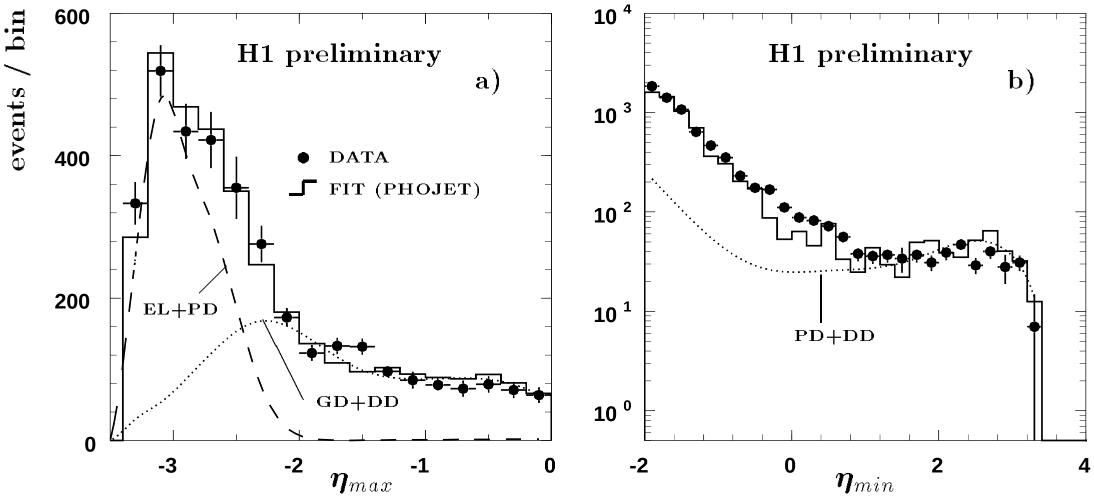

Figure 2: An example of a fit of (a) η_{max} and (b) η_{min} distributions with PHOJET Monte-Carlo (shifted-vertex data). σ_{DD} is fixed at 20 μb. Separately shown in (a) are the fitted contributions of elastic + p-diffraction (dashed curve) and gamma + double diffractions (dotted). Similary, in (b): proton + double diffractions (dotted).

We then fit with Eq.1 simultaneosly two event distributions *(i)* in η_{max} , η_{max} <0, *(ii)* in η_{min} , and *(iii)* the total number of of selected events. The σ_{DD} is fixed while σ_{ND}, σ_{GD}, σ_{PD}, σ_{EL} are free parameters determined in a fit.

An example of a fit with σ_{DD} =20 μb and PHOJET Monte-Carlo is shown in Fig.2. The fit describes the data reasonably well. There are *three important regions* in these plots. *The first region* is a plateau in the η_{max} distribution at $\eta_{max}\gtrsim-2$, dominated by γ- and double diffraction, which have practically identical shapes in terms of η_{max}. *The second region* is a bump at $\eta_{max}\lesssim-2$, populated mainly by p-diffraction and elastic events, again indistinguishable in shape. These events are primarily selected due to a single BPC-hit by a π meson from the decay of a vector meson emitted in these reactions in a direction close to that of γ . *The third region* is a plateau in the η_{min} distribution at $\eta_{min}\gtrsim1$ as dominated by p- and double diffraction. These three regions provide 3 basic constraints for 4 unknowns, and the 4th one comes from the total number of events.

The results on σ_{GD}, σ_{PD},σ_{EL} as a function of σ_{DD}, as obtained with PHOJET MC, are shown in Fig.3a in a wide range of σ_{DD}=0–40 μb. The shown errors are mostly due to the estimated model dependence while statistical errors are negligible. The model dependence was studied by varying **(a)** the MC generator PHOJET→PYTHIA; then, inside a generator, **(b)** the slopes b in $d\sigma/dt \sim e^{bt}$ for diffractive channels by factor 1.5, **(c)** the threshold value of M_X in GD : 1.0→1.2 GeV **(d)** the power p in $d\sigma/dM_X^2 \sim 1/M_X^p$: p =2→2.2 . The resulting variations of σ_i were added in quadrature to systematic errors.

One can see that the elastic cross section is almost independent of the assumption on σ_{DD} . γ- and p-diffraction show a stronger correlation with σ_{DD} . We observe

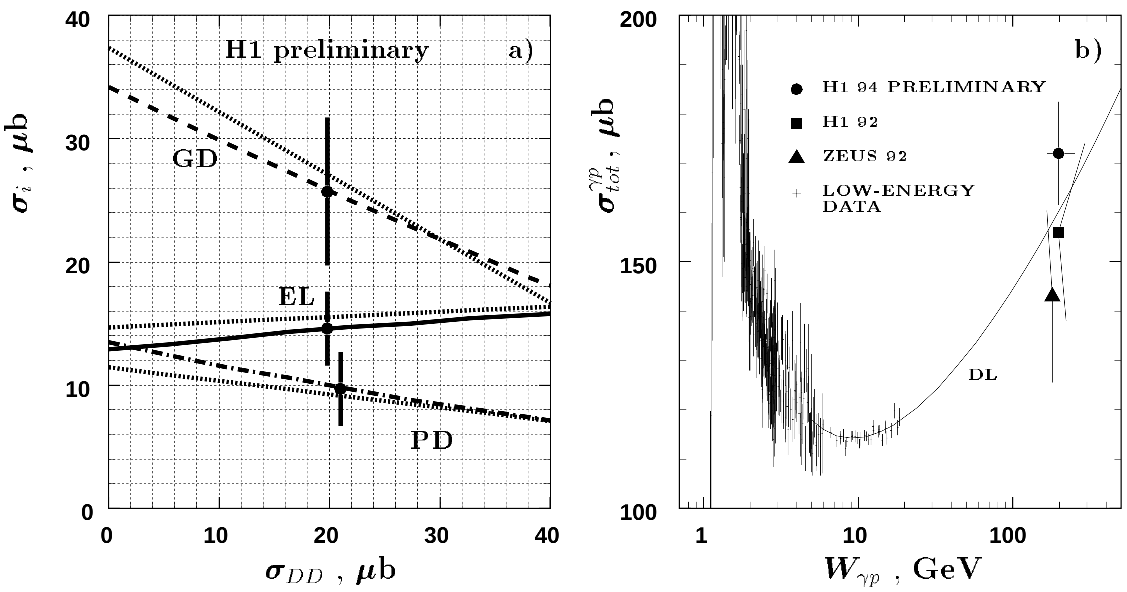

Figure 3: **(a)** Cross sections of elastic, gamma and proton diffraction as a function of double-diffraction cross section. Full, dashed and dash-dotted lines are obtained with the shifted-vertex data sample, dotted lines represent the nominal-vertex data. The shown errors are typical for any value of σ_{DD}. **(b)** Comparison of the $\sigma_{tot}^{\gamma p}$ from this analysis (nominal vertex sample) with earlier HERA results by H1 [2] and ZEUS [3], and low-energy data [4]. The curve is the Regge-model prediction by Donnachie-Landshoff [10].

that γ-diffraction is about 2 times larger than p-diffraction which is in contrast to the assumption of their equality made in earlier $\sigma_{tot}^{\gamma p}$ analyses [2,3] at HERA.

$\sigma_{tot}^{\gamma p}$ turns out to be remarkably insensitive to both σ_{DD} variation ($\sim$1% change) and model variations ($\sim$2% effect). This is easily explained by the fact that the overall efficiencies ε_i to different channels are quite close to each other, therefore, any possible migrations between the channels do not play any substantial role. We obtain

$$\sigma_{tot}^{\gamma p} = 171 \pm 3(\text{stat}) \pm 15(\text{syst})\ \mu\text{b}\ .$$

The systematic error is dominated by a 5.6% uncertainty in luminosity measurement and a 5% uncertainty of e-tagger acceptance. The *radiative corrections* have been taken into account for current experimental conditions based on calculation with HERACLES program [9], the applied correction to $\sigma_{tot}^{\gamma p}$ is equal to $+1\pm1\%$.

4.2 Nominal vertex sample

A similar analysis was performed for the data sample taken with the nominal position of interaction vertex. As compared to the first analysis, the main distinction consisted in the usage of another signature for events without tracks: instead of a BPC-hit, an energy deposition greater than 1 GeV in the backward calorimeter was required, see Fig.1 . Events with tracks were used to study η_{max} and η_{min} distributions. The overall efficiencies for this sample are given in the following table.

channel	ND	GD	PD	DD	EL
ε	.65	.66	.32	.66	.25

The found dependences of σ_{GD}, σ_{PD},σ_{EL} on σ_{DD} are shown in Fig.3a together with those from the first analysis and agree well with them.

The result on $\sigma_{tot}^{\gamma p}$ is also consistent:

$$\sigma_{tot}^{\gamma p} = 172 \pm 3(\mathrm{stat}) \pm 10(\mathrm{syst})\ \mu\mathrm{b}\ ,$$

being more precise due to a smaller error of luminosity measurement for this sample. The systematic error is dominated here by a 5% uncertainty of e-tagger acceptance. As compared to the first analysis, the result is more sensitive to the choice of the MC generator because of a lower acceptance to the elastic and p diffraction channels. The values got with PYTHIA and PHOJET differed by 4.6%. The central value is given above, with the 2.3% uncertainty included into the systematic error.

The new $\sigma_{tot}^{\gamma p}$ measurement is compared with earlier HERA results in Fig.3b. It agrees with the previous H1 value [2] but lies somewhat higher than the ZEUS one [3]. It still does not contradict to the phenomenological Regge-motivated prediction by Donnachie-Landshoff [10] where the speed of growth of the cross section with energy is assumed to be the same as the one observed in hadron-hadron interactions.

5. Summary

With H1 detector at HERA, the following preliminary results on γp scattering at the average c.m. energy of 197 GeV are obtained from the 1994 data. The correlation of γ-diffraction, p-diffraction and elastic cross sections with double-diffraction cross section is determined. The cross section of γ diffraction is substantially greater than the p-diffraction cross section. The measured total cross section is equal to 172 $\pm$ 3(stat) $\pm$ 10(syst) μb with the noticeably smaller uncertainty as compared to earlier HERA results.

References

1. C.F.Weizsäcker, *Z.Phys.***88** (1934)612; E.J.Williams, *Phys.Rev.***45** (1934)729; S.Frixione *et al., Phys.Lett.* **B319**(1993)339.
2. H1 collab.,T.Ahmed *et al., Phys.Lett.***B299**(1993)374; S.Levonian, in *Proc. of the XXVIIIth Rencontre de Moriond* (1993),p.529.
3. ZEUS collab.,M.Derrick *et al., Z.Phys.***C63**(1994)391.
4. A.Baldini *et al., Landolt-Börnstein's New Series* v.**I/12b** (1988), p.347.
5. H1 collab.,I.Abt *et al., DESY preprint* 93-173(1993), to be published in *NIM.*
6. H1 collab.,T.Ahmed *et al., DESY preprint* 95-024(1995), to be published in *Z.Phys.*
7. T.Sjöstrand,*CERN-TH*-6488(1992).
8. R.Engel, in *Proc. of the XXIXth Rencontre de Moriond* (1994),p.321.
9. A.Kwiatkowski,H.Spiesberger,H.-J.Möring, in *Proc. of the Workshop "Physics at HERA"*(1993),v.**3**,p.1294.
10. A.Donnachie,P.V.Landshoff,*Phys.Lett.***B296**(1992)227.